DELINEATION OF FAULT ZONES USING IMAGING RADAR

M. N. Toksoz, L. Gulen, M. Prange, and J. Matarese
Earth Resources Laboratory
Department of Earth, Atmospheric, and Planetary Sciences
Massachusetts Institute of Technology
Cambridge, Massachusetts

G. H. Pettengill and P. G. Ford
Center for Space Research
Massachusetts Institute of Technology
Cambridge, Massachusetts

The assessment of earthquake hazards and mineral and oil potential of a given region requires a detailed knowledge of geological structure, including the configuration of faults. Delineation of faults is traditionally based on three types of data: 1) seismicity data, which shows the location and magnitude of earthquake activity; 2) field mapping, which in remote areas is typically incomplete and of insufficient accuracy; and 3) remote sensing, including Landsat images and high altitude photography. Recently, high resolution radar images of tectonically active regions have been obtained by SEASAT and Shuttle Imaging Radar (SIR-A and SIR-B) systems. These radar images are sensitive to terrain slope variations and emphasize the topographic signatures of fault zones. Our objective is to develop techniques for using the radar data in conjunction with the traditional types of data to delineate major faults in well-known test sites, and to extend interpretation techniques to remote areas.

Two study areas in this paper cover the tectonically complex region of Southern California, including the San Andreas and Garlock faults around the Mojave plate, and an equally complex region in Turkey, containing the North Anatolian Fault zone. In both of these areas extensive geological and seismic data are available and are being collected by ongoing studies. An excellent example of the sensitivity of imaging radar to the morphological features of major fault zones is shown by a SEASAT image of the Mojave plate (Figure 1a). A qualitative fault interpretation of Figure 1a is given in Figure 1b. Major fault zones such as the San Andreas, Garlock, and San Gabriel, along with the associated secondary faults, can be clearly identified on SEASAT imagery. The most striking features of these faults on the radar imagery are long, linear valleys and scarps. Also associated with these linear features are discontinuities created by offset streams, ridges, and valleys. These discontinuities are necessary to identify faults among other linear features. Radar imagery yields high resolution textural information unavailable on Landsat images. An example of such textural information is given by the contrast between the Mojave plate and surrounding regions on Figure 1a.

The fault zones on radar imagery can be delineated by identifying the above characteristics using digital techniques. The digital techniques that we use for fault detection consist of edge detectors as pre-processors and line detectors as post-processors. We are currently exploring two techniques: a smoothed directional derivative filter (Canny, 1983), and Kalman filtering. A derivative filter emphasizes various frequency components

of an image along a given direction, making edges appear as spikes. We operate the filter in twelve cardinal directions, yielding directional and edge magnitude information at each pixel. The Kalman filter tracks statistics (such as mean and variance) within an expanding window and indicates edges where the window encounters points which do not match these statistics. The advantage of Kalman filtering is that any statistical parameters may be used for the edge detection criteria; however, no directional information is generated.

The post-processors are methods for finding lines in the edge detector output. We are evaluating three techniques: a gun-sight line finder, a linking line finder (Nevatia and Babu, 1978), and simulated annealing (Geman and Geman, 1984; Derin et al., 1984). The gun-sight line finder examines thresholded edge magnitudes and directional deviations along a given direction, putting linear segments where the point density is above a given value. The linking line finder is a connect-the-dots algorithm which uses directional information at each point to trace curvilinear segments, ending a segment where the directional deviation is above a threshold. The simulated annealing method emplaces line elements using edge magnitude and directional information, and then tests the global energy of this line configuration according to an a priori energy function, and iterates over the line segment configuration to minimize this energy. An efficient line finder will ultimately be a combination of these basic algorithms.

The usefulness of the above techniques was demonstrated by the delineation of a previously unknown active fault zone in a remote area in eastern Turkey using the SIR-A image in Figure 2a. Three large earthquakes (M_b>5) and a number of smaller aftershocks were recorded near Olur in 1983 and 1984. For fault detection, the gun-sight line finder was applied to derivative filter output and the result is shown in Figure 2a. The fault, which is difficult to detect by eye on the SIR-A image, is greatly enhanced by the processing. The seismicity data obtained by the seismic network that we set up to monitor this recent earthquake activity is shown in Figure 2b. The alignment of earthquake epicenters along the Olur fault verifies our SIR-A interpretation.

Digital processing is also being applied to a SIR-B image covering an area in Southern California at the intersection of the San Andreas and Garlock fault zones (Figure 3a). A qualitative fault interpretation of this image is shown in Figure 3b. The faults in this area are curvilinear on a small scale, making the gun-sight approach ineffective. An example of the linking line finder applied to the derivative filtered image is shown in Figure 3c. This method successfully delineates the San Andreas, Garlock, and Pine Mountain fault zones. We are currently working to improve the fault detection technique by using a combination of the above algorithms, including a texture sensitive pre-processor.

REFERENCES

Canny, J. (1983), Finding Edges and Lines in Images, MIT Artificial Intelligence Laboratory, Technical Report No. 720.

Derin, H., H. Elliot, R. Cristi, and D. Geman, (1984), Bayes smoothing algorithms for segmentation of binary images modeled by Markov random fields, IEEE Trans. Pattern Anal. Machine Intell.

Geman, D., and S. Geman, (1984), Stochastic relaxation, Gibbs distribution, and Bayesian restoration of images, IEEE Trans. Pattern Anal. Machine Intell.

Nevatia, R., and K. Babu, (November, 1978), Linear feature extraction, Proceedings of the Image Understanding Workshop, ed. Bauman Lee, Science Applications.

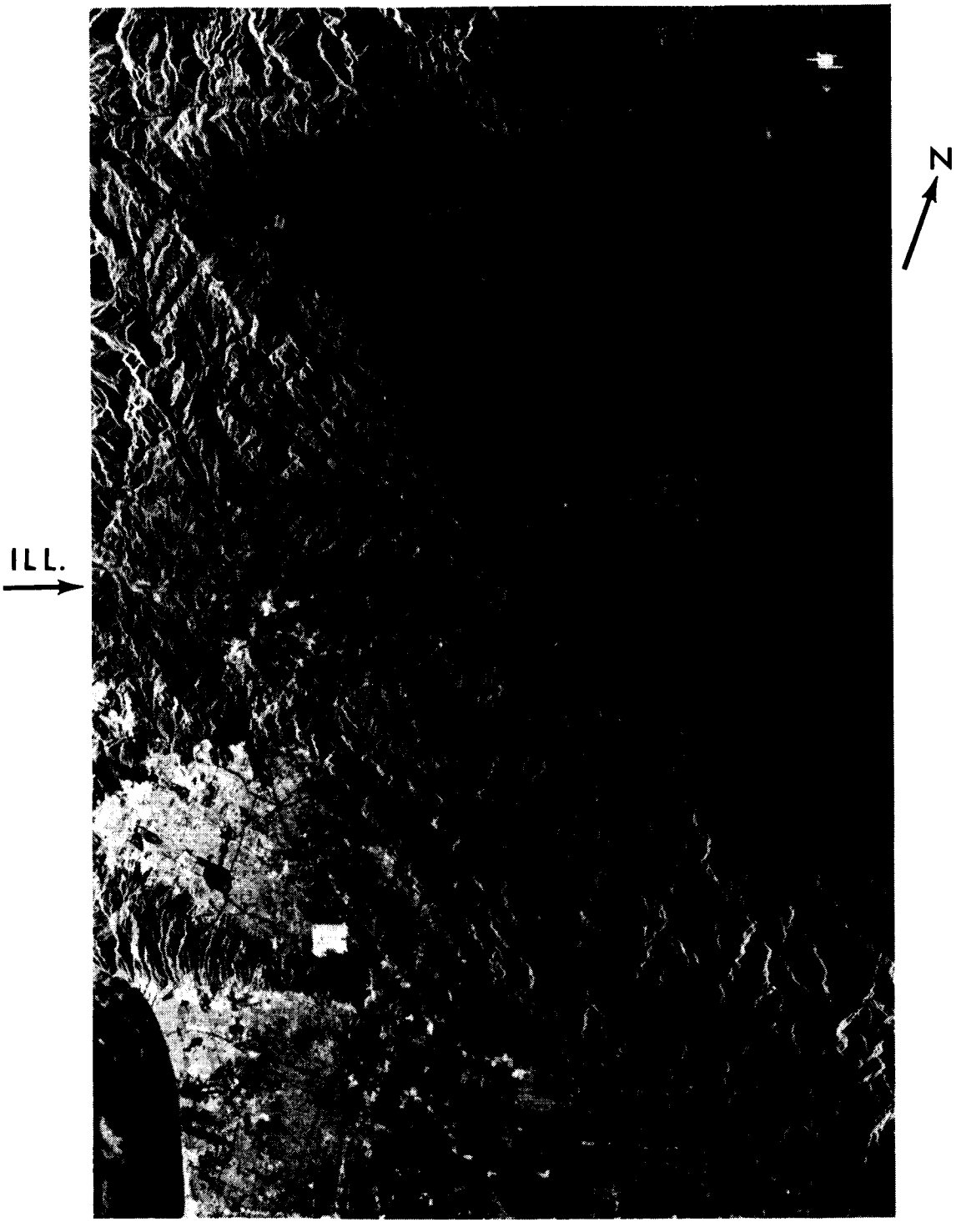

Figure 1a. Composite SEASAT radar (23.5cm wavelength) image of Southern California.

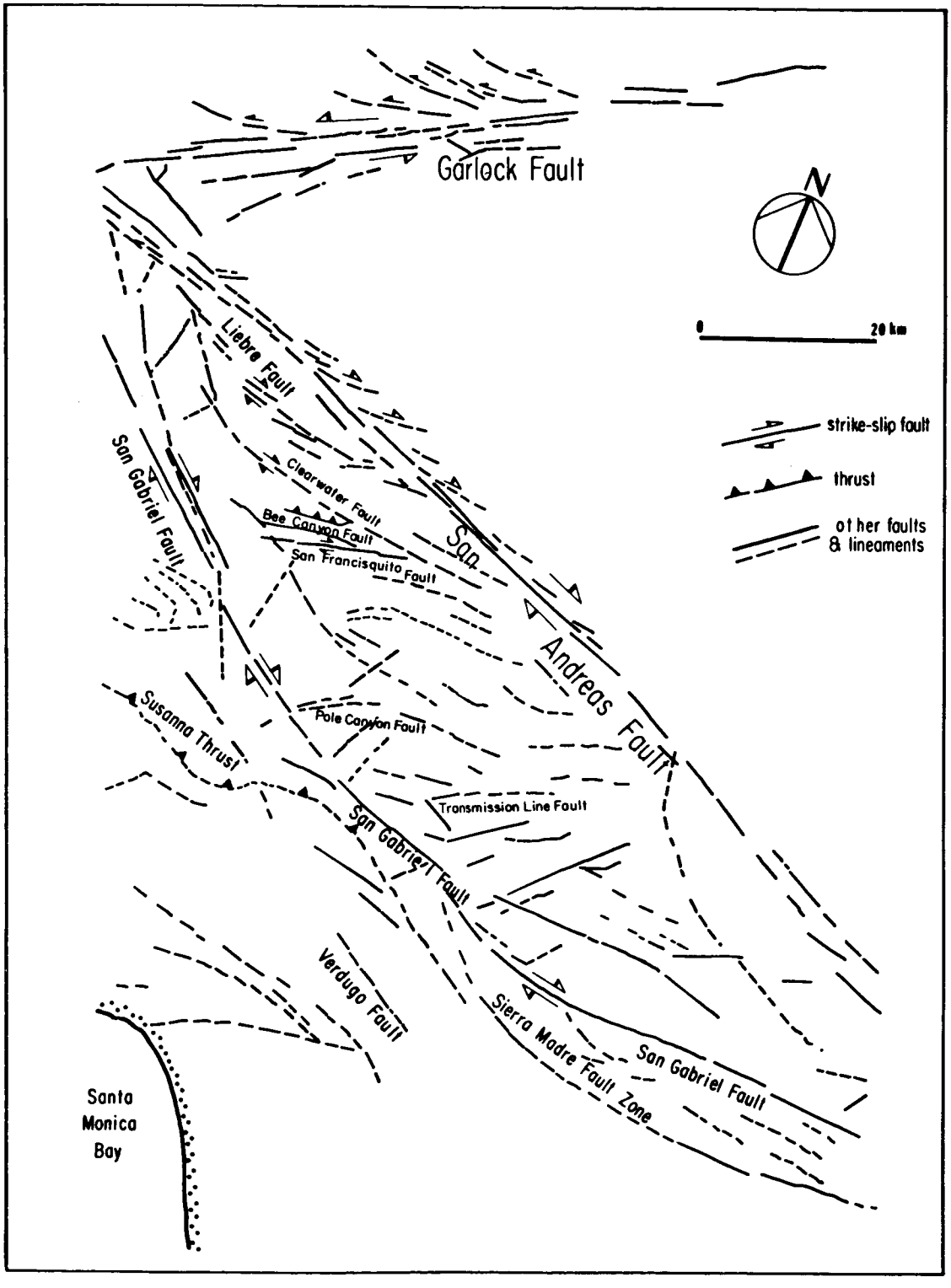

Figure 1b. Qualitative fault interpretation of Figure 1a.

Figure 2a. SIR-A image of Olur area with superimposed digital fault interpretation showing Olur fault.

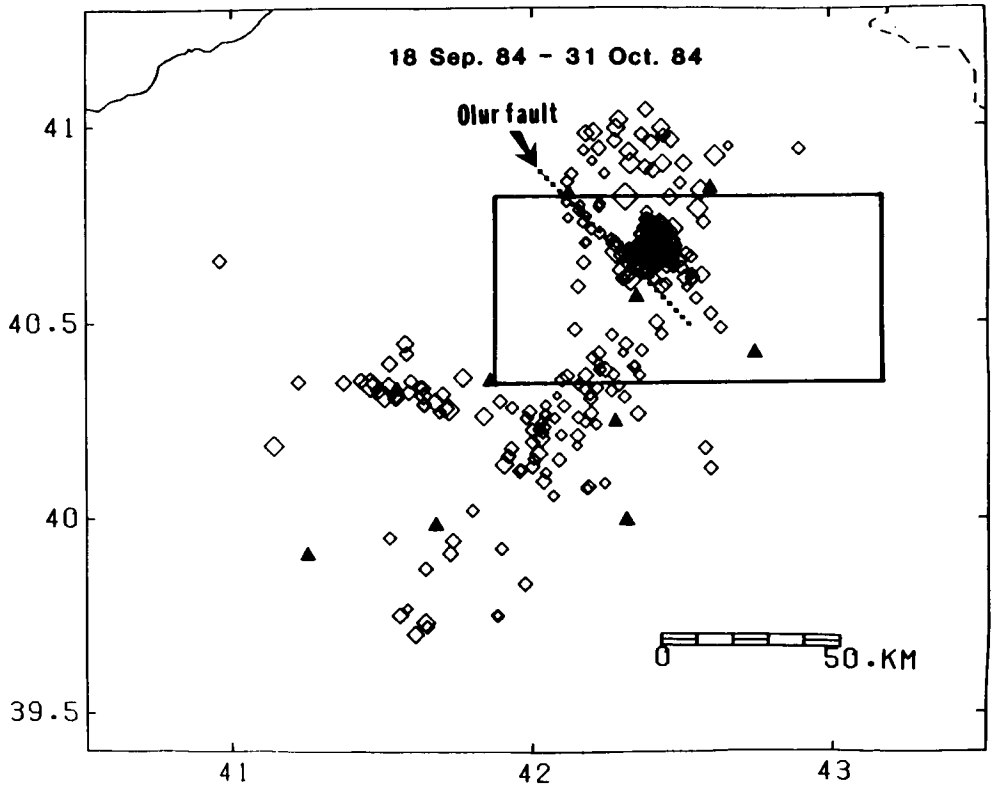

Figure 2b. Distribution of aftershock epicenters in the Olur area in the period 18 Sept. 1984 to 31 Oct. 1984, with the box indicating the area covered by the SIR-A image in Figure 2a. The filled triangles indicate the location of seismic stations. The open diamonds denote the epicenters of aftershocks, and size indicates relative magnitude. The NE-SW alignment of epicenters verifies the digital SIR-A Olur fault interpretation.

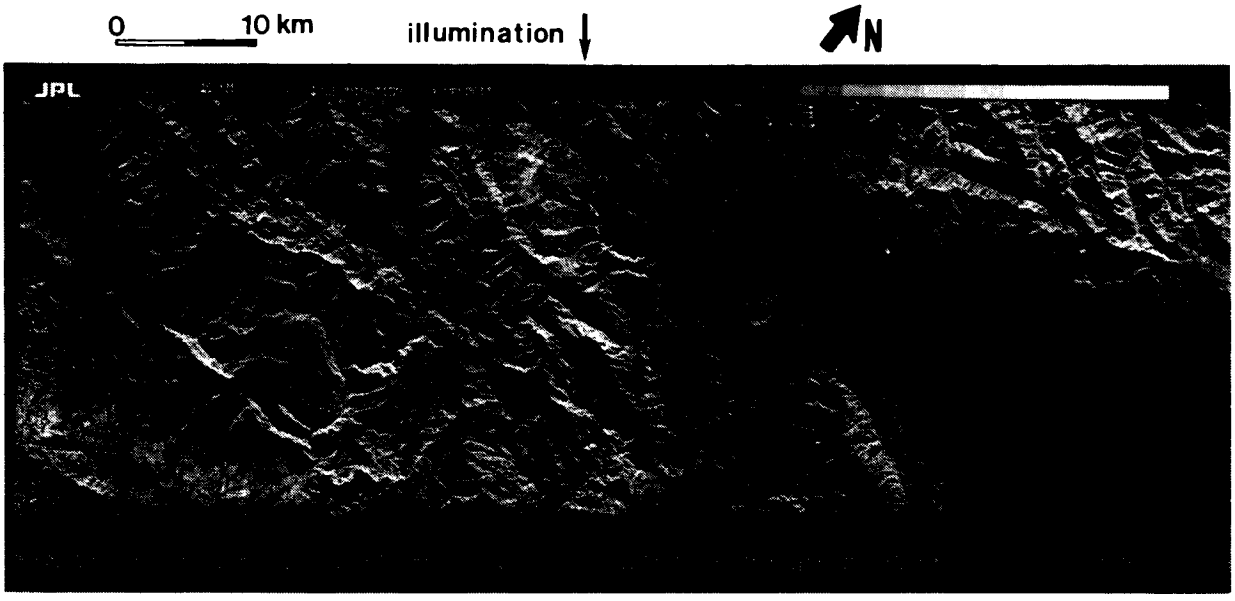

Figure 3a. SIR-B image covering an area in Southern California at the intersection of the San Andreas and Garlock fault zones.

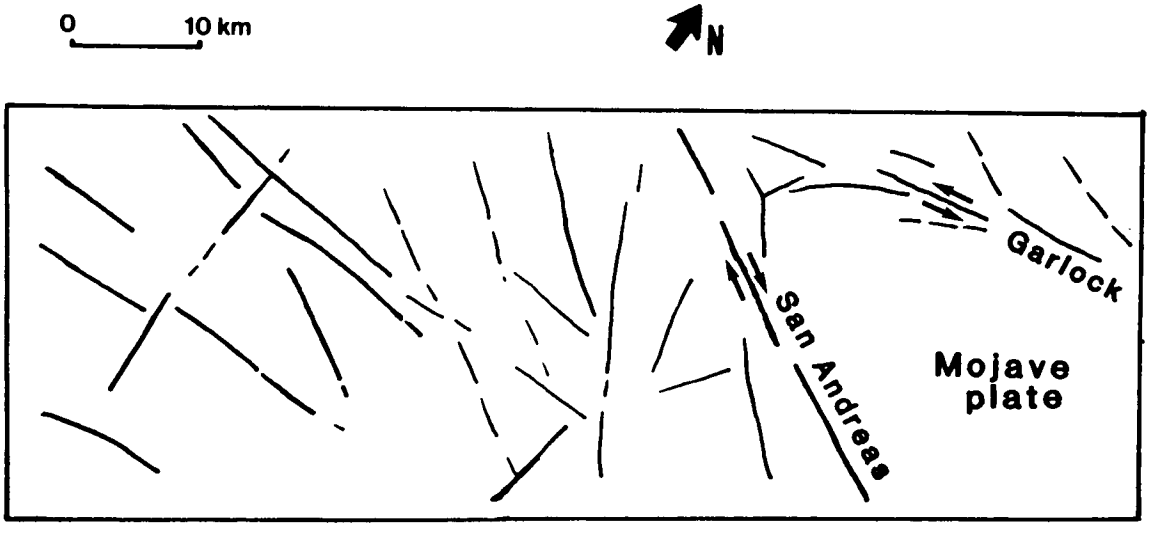

Figure 3b. The qualitative fault interpretation of Figure 3a.

Figure 3c. A digital fault interpretation of Figure 3a using the linking line finder applied to the derivative filtered SIR-B image. The SIR-B image was smoothed by pixel averaging before processing. This method successfully delineates the San Andreas, Garlock, and Pine Mountain fault zones.